Large built-in electric fields due to flexoelectricity in compositionally graded ferroelectric thin films

J. Karthik, R. V. K. Mangalam, J. C. Agar, and L. W. Martin*

Department of Materials Science and Engineering and Materials Research Laboratory, University of Illinois, Urbana-Champaign, Urbana, Illinois 61801, USA

(Received 14 October 2012; revised manuscript received 21 December 2012; published 30 January 2013)

We investigate the origin of large built-in electric fields that have been reported in compositionally graded ferroelectric thin films using $PbZr_{1-x}Ti_xO_3$ ($0.2 < x < 0.8$) as a model system. We show that the built-in electric fields that cause a voltage offset in the hysteresis loops are dependent on strain relaxation (through misfit dislocation formation) and the accompanying polarization distribution within the material. Using a Ginzburg-Landau-Devonshire phenomenological formalism that includes the effects of compositional gradients, mechanical strain relaxation, and flexoelectricity, we demonstrate that the flexoelectric coupling between the out-of-plane polarization and the gradient of the epitaxial strain throughout the thickness of the film, not other inhomogeneities (i.e., composition or polarization), is directly responsible for the observed voltage offsets. This work demonstrates the importance of flexoelectricity in influencing the properties of ferroelectric thin films and provides a powerful mechanism to control their properties.

DOI: 10.1103/PhysRevB.87.024111 PACS number(s): 77.55.fg, 77.22.Ej, 77.80.bg, 77.80.bn

I. INTRODUCTION

Ferroelectric materials have broken inversion symmetry at the unit cell level. Bilayer and compositionally graded thin-film ferroelectric heterostructures additionally have macroscopic broken inversion symmetry across the thickness of the material. Such macroscopic inversion symmetry breaking and the associated novel physical properties have attracted widespread experimental and theoretical attention in the past decade. In contrast to single-component ferroelectrics, the degeneracy between the two polarization states in these materials is broken by a built-in electric field, which has been shown to result in self-poling,[1] shifted hysteresis loops,[2,3] enhanced susceptibilities,[4–7] and signatures of geometric frustration.[8] Such a built-in bias within the material is typically generated by an inhomogeneous strain through lattice engineering (via multicomponent superlattices)[9,10] or a global composition gradient.[1–6] Since the built-in fields can result in enhanced susceptibilities and directly affect the polarization switching characteristics, understanding the origin of the observed behavior is key to utilizing it in practical applications such as nonvolatile memories, piezoelectric sensors, and thermal imaging systems. In spite of extensive theoretical[4,11–13] and experimental[1–7] studies on compositionally graded ferroelectric heterostructures over the last two decades, the physical mechanism behind the built-in fields has been difficult to identify due to a plethora of intrinsic and extrinsic factors that have been proposed to give rise to the observed behavior.

Early experiments on compositionally graded heterostructures reported a shift in the polarization (vertical) axis of the hysteresis loops and gradients in the polarization within the material were believed to cause the observed offsets.[3,6] The measured vertical offsets, however, were explicitly dependent on the measurement circuit (i.e., the reference capacitor of the Sawyer-Tower circuit and the applied voltage)[6,14] and exhibited an exponential approach to a stable equilibrium offset after the application of an electric field. The measured polarization, in turn, corresponded to physically unrealistic values (i.e., $>250\ \mu C/cm^2$ in compositionally graded $PbZr_{1-x}Ti_xO_3$ films).[2,15] Later work[16] indicated that these observed shifts should, in fact, be along the voltage (horizontal) axis due to a built-in electric field, but can be manifested as a polarization offset in a hysteresis measurement under certain measurement configurations. These shifts are distinctly different from shifts in hysteresis loops that arise from extrinsic effects such as asymmetric electrodes[17] or the inhomogeneous distribution of oxygen vacancies[15] in the capacitor. The effects of interest are intrinsic to the material and result from the macroscopic broken inversion symmetry. Further, theoretical work has also pointed out that apart from a polarization gradient, inhomogeneities in composition and strain[18] can also play a role in generating a symmetry breaking internal field.[19–21] In particular, flexoelectric coupling (which relates polarization and strain gradients in a material) has been recently shown to significantly affect the properties of ferroelectrics, particularly in thin films with large strain gradients due to structural relaxation via misfit dislocation formation[22–24] and near surfaces and interfaces.[25,26] This is primarily due to the much larger strain gradients that can be sustained in thin films ($>10^5\ m^{-1}$)[24] as compared to that which is possible in bulk crystals or sintered ceramic materials ($<1\ m^{-1}$).[19] The effects of composition variation, structural relaxation, strain gradients, and flexoelectric coupling, however, have not been addressed in any study of compositionally graded ferroelectric thin films although these effects are certainly present and likely greatly impact the properties of such systems.

In this study, we perform a detailed investigation of the voltage offsets in compositionally graded $PbZr_{1-x}Ti_xO_3$ (PZT) thin films using Ginzburg-Landau-Devonshire (GLD) theory. Our work indicates that the observed physical properties of such films are the result of a delicate interplay between strain relaxation due to misfit dislocation formation, the polarization distribution within the film, and flexoelectric interactions. The experimentally observed ferroelectric hysteresis and comparisons to GLD models reveal that the built-in electric field is intrinsic to the compositionally graded thin film and is a direct consequence of the strong flexoelectric coupling between the out-of-plane polarization and the in-plane epitaxial strain.

 ©2013 American Physical Society

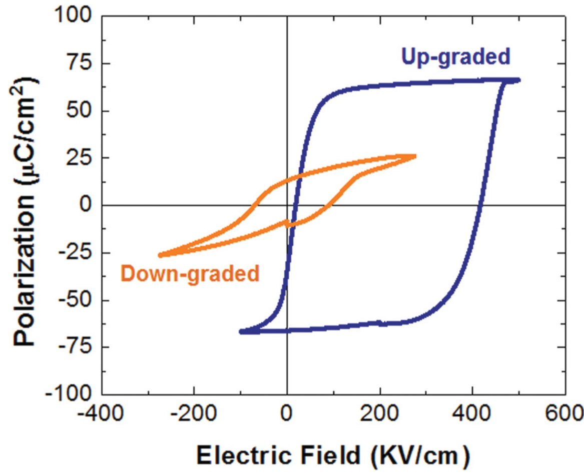

FIG. 1. (Color online) Ferroelectric hysteresis loops obtained at 1 kHz for compositionally up-graded and down-graded thin films.

II. EXPERIMENTAL OBSERVATIONS

We focus on model 100 nm thick, compositionally graded heterostructures of $PbZr_{1-x}Ti_xO_3$ with end members $x = 0.2$ (a rhombohedral ferroelectric with lattice parameter $a = 4.118$ Å and $\alpha = 89.73^\circ$) and $x = 0.8$ (a tetragonal ferroelectric with lattice constants $a = 3.94$ Å and $c = 4.12$ Å). For the models, we assume epitaxial growth of the films on single crystal $GdScO_3$ substrates (orthorhombic, with an average in-plane lattice parameter $a = 3.97$ Å), which have a lattice mismatch of $+0.8\%$ (tensile) and -3.5% (compressive) with the $PbZr_{0.2}Ti_{0.8}O_3$ and $PbZr_{0.8}Ti_{0.2}O_3$, respectively. We explore two model heterostructures: (1) compositionally up-graded heterostructures (which smoothly transition from $PbZr_{0.2}Ti_{0.8}O_3$ to $PbZr_{0.8}Ti_{0.2}O_3$ from the substrate to the film surface) and (2) compositionally downgraded heterostructures (which smoothly transition from $PbZr_{0.8}Ti_{0.2}O_3$ to $PbZr_{0.2}Ti_{0.8}O_3$ from the substrate to the film surface).

The motivation for this study is the observation of intriguing differences in the nature of ferroelectric response between these different heterostructures.[27] Ferroelectric hysteresis loops (measured at 1 kHz) for the two different compositionally graded heterostructures reveal dramatically different behavior (Fig. 1). Hysteresis loops obtained from compositionally up-graded heterostructures reveal large saturation and remnant polarization, square hysteresis loops, and a large voltage offset while those from down-graded heterostructures reveal low saturation and remnant polarization, slanted hysteresis, and no voltage offsets. At first glance, the films should both possess the same magnitude of composition and polarization gradient across the thickness of the film and, therefore, the presence of a voltage offset in the compositionally up-graded thin film alone is unexpected. In reality, vastly different compatibility between the various phases and the substrate, changes in crystal structure and symmetry, and corresponding variations in polarization likely combine to result in a complex and potentially unexpected manifestation of unusual structural and ferroelectric properties. The current study is meant to develop a physical picture of the interplay of strain and strain relaxation, structural evolution, and polarization in these novel heterostructures and to provide insights as to the driving force for voltage offsets in some heterostructures and not others.

III. MODELING OF COMPOSITIONALLY GRADED FILMS

To rationalize the observed ferroelectric properties and understand the origin of the built-in fields, we utilized a GLD phenomenological model including the effects of local inhomogeneities in polarization (P) and stresses (σ), flexoelectric coupling between polarization and stress gradients, and misfit dislocation formation to provide a realistic theoretical foundation to understand compositionally graded ferroelectric heterostructures. For the case of epitaxially constrained thin films, the correct thermodynamic description is provided by a Legendre transformation of the Gibbs free energy density (G) as[26,28]

$$\tilde{G} = G + u_1\sigma_1 + u_2\sigma_2 + u_6\sigma_6, \tag{1}$$

where u_i and σ_i represent the strains and stresses, repectively (in the Voigt notation, with x_3 perpendicular to the film-substrate interface). For the case of monodomain (001)-oriented thin films grown on cubic substrates, G can be written as[26,29]

$$G(x_3) = \alpha_i P_i^2 + \alpha_{ij} P_i^2 P_j^2 + \alpha_{ijk} P_i^2 P_j^2 P_k^2 - s_{ijkl}\sigma_{ij}\sigma_{kl} - Q_{ijkl}\sigma_{ij} P_k P_l + g_{ijkl}\left(\frac{\partial P_i}{\partial x_j}\right)\left(\frac{\partial P_k}{\partial x_l}\right) + \frac{1}{2}\mu_{ijkl}\left(\sigma_{ij}\frac{\partial P_k}{\partial x_l} - P_k\frac{\partial \sigma_{ij}}{\partial x_l}\right); \quad i,j = 1-3, \tag{2}$$

where P_i are the polarization components, σ_{ij} are the components of the stress tensor, α_i, α_{ij}, and α_{ijk} represent the bulk stiffness coefficients, s_{ijkl} are the components of the elastic compliance tensor, Q_{ijkl} are the electrostrictive coefficients, g_{ijkl} are the gradient energy coefficients, and μ_{ijkl} are the flexoelectric coefficients. The stiffness coefficients, elastic compliances, and electrostrictive coefficients for the $PbZr_{1-x}Ti_xO_3$ system were obtained from Refs. 30 and 31. The composition dependence of the material constants and the stiffness coefficients is reflected in a position dependence of all quantities except for the flexoelectric coupling and the gradient energy coefficients in Eq. (2). In the absence of experimental measurements of flexoelectric coupling in $PbZr_{1-x}Ti_xO_3$ as a function of composition, a constant value was used for the entire range of compositions studied here.[29] The gradient energy coefficients were taken as $g_{11} = 2 \times 10^{-10}$ $C^{-2}m^4N$ and $g_{44} = 1 \times 10^{-10}$ $C^{-2}m^4N$.[32] The depolarizing fields within the film are neglected due the thickness of our films [in this case, 100 nm, which is much larger than the screening length of standard oxide electrodes (∼1 Å)],[33] the presence of symmetric electrodes, and the finite conductivity of $PbZr_{1-x}Ti_xO_3$.[34] The free energy was supplemented by the relevant mechanical and electrical boundary conditions as shown below and minimized numerically to obtain the equilibrium state of the polarization and stress/strain within the film.

The stress components in Eq. (1) are obtained using $u_1 = u_2 = u$ and $u_6 = \sigma_3 = \sigma_4 = \sigma_5 = 0$, where $u_i = -\frac{\partial G}{\partial \sigma_i}$.[28] The total in-plane strain (u) within the film is a function of the distance x_3 away from the substrate interface and is different from the misfit strain [$u_m(x_3)$] with the substrate due to strain

relaxation. It should be noted that the misfit strain itself varies with x_3 due to the composition dependence of the lattice constants in $PbZr_{1-x}Ti_xO_3$[35] and is calculated as $u_m(x_3) = 1 - \frac{a_f(x_3)}{a_s}$, where a_f, a_s are the film and substrate lattice parameters, respectively. The compositional dependence of the lattice constants of $PbZr_{1-x}Ti_xO_3$ was obtained from Refs. 35 and 36.

Including the effect of misfit dislocation formation at a temperature T_g, the total strain can be obtained by minimizing the total strain energy.[37–39] This total strain energy per unit area (U) is given as

$$U = \int_0^t \left[Y\left(u_m \pm \int_0^{x_3} \rho b cos\lambda\right)^2 + G\frac{\rho|b|^2}{2\pi} \ln\left(\frac{t-x_3}{|b|}\right)\right] dx_3,$$

where the first term represents the reduction in energy due to misfit dislocation formation and the second term represents the energy cost of forming dislocations. In this equation, Y is the biaxial modulus, G is the shear modulus, t is the thickness of the film, ρ is the dislocation density, and b is the Burgers vector for the lowest energy dislocations (i.e., $\langle 110\rangle$ dislocations inclined at $\lambda = 45^\circ$ to the substrate).[38] The sign of b in the first term is chosen to reduce the misfit strain at that location with $|b| = \sqrt{2}a$. The equilibrium density of misfit dislocations and the total strain were obtained by minimizing U using a modified look-ahead minimizing scheme.[39]

Strain relaxation via misfit dislocation formation, as described above, has been studied previously for perovskite ferroelectrics assuming complete relaxation at the growth temperature and no further dislocation formation at lower temperatures.[38] Complementary work on semiconductor systems, however, typically assumes evolution of equilibrium dislocation distributions down to room temperature.[39] In reality, the actual distribution is likely bounded by these two extremes as dislocation formation is often kinetically limited and is not well understood for complex perovskite ferroelectrics grown in their paraelectric state such as the compositionally graded films used in this study. The equilibrium distribution of dislocations calculated above provides a good starting point for the theoretical analysis of the strain relaxation during the synthesis of such compositionally graded heterostructures.[37] To tackle this ambiguity in our understanding of the relaxation processes, we calculated the dislocation density and strain distribution at $T_g = 800$ and 300 K. Additionally, there are different approaches to the definition of the elastic moduli (Y and G) for the different defect formation processes. As per existing models of strain relaxation[38,39] two cases were considered for the elastic stiffness: (1) $Y = C_{11} + C_{12} - 2C_{12}^2/C_{11}$, $G = (C_{11} - C_{12})/2$ (henceforth referred as $Y > G$) and (2) $Y = G = C_{11} + C_{12} - 2C_{12}^2/C_{11}$ (henceforth referred to as $Y = G$), where C_{ij} are the components of the elastic stiffness tensor. Finally, the strain distribution for dislocation formation at $T_g = 300$ K is given by $u(x_3) = u_m(x_3) \pm \int_0^{x_3} \rho b \cos\lambda$. It should be noted that calculations at $T_g \neq 300$ K must be appropriately scaled due to thermal expansion of the substrate and the film. In this case, the misfit strain at T_g is relaxed by dislocation formation at that temperature and the final total strain at room temperature (T_r) is calculated as $u(x_3,T_r) = 1 - \frac{a_f(x_3)}{a_s^*(x_3,T_r)}$, where $a_s^*(x_3,T_r) = a_s^*(x_3,T_g)[1 + \alpha_s(T_r - T_g)]$,[35] where $a_s^*(x_3,T_g) = a_s(T_g)\frac{1-u_m(x_3,T_g)}{1-u(x_3,T_g)}$ and

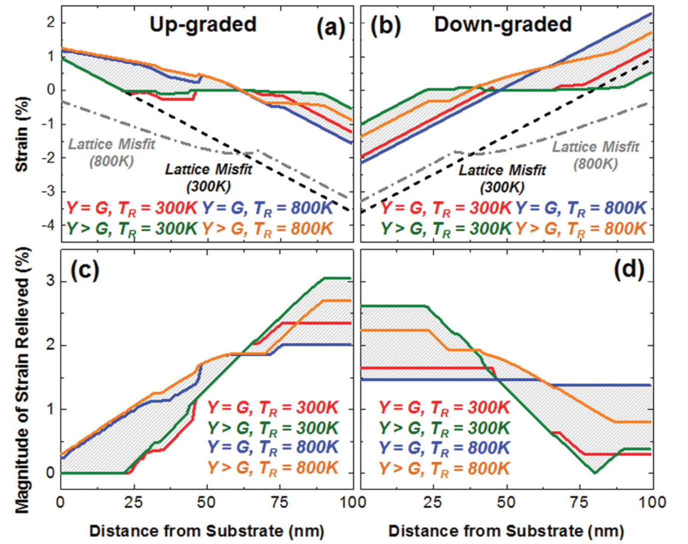

FIG. 2. (Color online) Evolution of strain in compositionally graded thin films including the theoretical lattice misfit strain (u_m) at 300 K (black dashed line) and 800 K (grey dash-dot line) as well as the total strain (u) at 300 K (as calculated by the various model variants) for compositionally (a) up-graded and (b) down-graded thin films. The magnitude of the strain relieved by dislocation formation ($|u - u_m|$) is also shown for compositionally (c) up-graded and (d) down-graded films. The four model variants considered are $Y = G$, $T_g = 300$ K (red), $Y > G$, $T_g = 300$ K (green), $Y = G$, $T_g = 800$ K (blue), and $Y > G$, $T_g = 800$ K (orange) and the striped grey regions represent the values bounded by the various models.

α_s is the thermal expansion coefficient of the substrate. The thermal expansion coefficients for the $GdScO_3(110)$ substrate and $PbZr_{1-x}Ti_xO_3$ film were taken as 12×10^{-6} K^{-1} and 5.4×10^{-6} K^{-1}, respectively.[40] Thus we considered four model variations: (1) strain relaxation at high temperatures only with equivalent moduli ($Y = G$, $T_g = 800$ K), (2) strain relaxation at high-temperatures with different moduli ($Y > G$, $T_g = 800$ K), (3) strain relaxation down to room temperature with equivalent moduli ($Y = G$, $T_g = 300$ K), (4) strain relaxation down to room-temperature with different moduli ($Y > G$, $T_g = 300$ K) (Fig. 2). For comparison, the unrelaxed lattice misfit strain $[u_m(x_3)]$ calculated both at 300 and 800 K is provided.

IV. RESUTS AND DISCUSSION

For all model variations studied, we find that the overall trends follow, unsurprisingly, the nature of the lattice mismatch. The shaded areas in Fig. 2 represent the range of expected results as bounded by the various models. For the compositionally up-graded heterostructure [Fig. 2(a)], there is a significant substrate induced compressive strain retained throughout the thickness of the film. In contrast, the formation of a high density of dislocations at the film-substrate interface (calculated dislocation densities are as large as 10^{16}–10^{17} m^{-2}) results in significant strain relaxation in the compositionally down-graded heterostructure [Fig. 2(b)]. As a result, a large fraction of the down-graded film is placed under tensile strain due to the large in-plane lattice parameter of the relaxed Zr-rich underlayer, which screens the Ti-rich region from the

substrate lattice. This trend is further clarified by examining the magnitude of the strain relieved via dislocation formation [i.e., $|u(x_3) - u_m(x_3)|$] for both the up-graded and down-graded thin films [Figs. 2(c) and 2(d)]. A significantly smaller amount of the strain is relieved near the substrate interface for the up-graded film (~0.2%) as compared to the down-graded film (~2%). This is supported by the dislocation density extracted from the models, which suggests that down-graded films possess a dislocation density nearly two orders of magnitude larger than that of the up-graded films in the near interface limit. Furthermore, despite minor variations in the calculated strain distribution between the various models, the simulations identify an important trend—the structural compatibility of the bottom-most layer and the substrate plays a crucial role in determining the overall strain distribution in the heterostructure. From this analysis, it is found that the compositionally up-graded heterostructures possess an overall compressive strain and are generally less relaxed due to the better structural compatibility with the substrate. The compositionally down-graded heterostructures, on the other hand, relax rapidly near the substrate (due to a large misfit strain) through misfit dislocation formation and as a result, have an overall tensile strain over the majority of the film. This insight is confirmed by structural characterization of the heterostructures by x-ray reciprocal space mapping studies [see Figs. S1(a) and S1(b) in Supplemental Material],[41] which reveal that the compositionally up-graded heterostructures are more coherently strained to the substrate throughout the film thickness while the compositionally down-graded heterostructures reveal relaxed phases.

To understand how this strain distribution affects the polarization within the films, the GLD free energy in Eq. (1) was minimized numerically with the total strain distribution. The usual boundary condition for the polarization components P_i is modified by flexoelectricity and, for the case of short-circuited thin films, acquires the form[26,29,42]

$$n_3 g_{44}\frac{\partial P_i}{\partial x_3} + n_3\frac{\mu_{12}P_iP_3(Q_{11}+Q_{12})}{s_{11}+s_{12}} + g_{44}\frac{P_i}{\delta} = 0; \quad i = 1,2$$

$$n_3\left(g_{11}+\frac{\mu_{12}^2}{s_{11}+s_{12}}\right)\frac{\partial P_3}{\partial x_3} + n_3\frac{\mu_{12}u_s}{s_{11}+s_{12}} - n_3\frac{\mu_{12}\{(Q_{11}+Q_{12})(P_1^2+P_2^2)+2Q_{12}P_3^2\}}{2(s_{11}+s_{12})} + g_{11}\frac{P_3}{\delta} = 0,$$

where n_3 is the unit vector along the surface normal, δ is the extrapolation length at the surface, and u_s is the value of the in-plane strain at the boundary (i.e., $x_3 = 0, 100\,\text{nm}$). Upon solving the equations of state for polarization in three dimensions, we observe that for compositionally up-graded heterostructures that as one transitions from the film-substrate interface to the film surface, the increasing compressive strain in the film causes the in-plane polarization ($P_1 = P_2$) [Fig. 3(a)] to reduce and the out-of-plane polarization (P_3) [Fig. 3(b)] to increase. This is unexpected since the top-most portion of the film should possess a rhombohedral-like crystal structure with strong in-plane polarization components. The models suggest that compositionally grading the heterostructure allows one to quench the in-plane polarization at the expense of out-of-plane polarization in these heterostructures. In the case of compositionally down-graded heterostructures, on the other hand, as one transitions from the film-substrate interface to the film surface, the increasing tensile strain in the film causes the in-plane polarization ($P_1 = P_2$) to increase [Fig. 4(a)] and the out-of-plane polarization (P_3) to decrease [Fig. 4(b)]. In fact, the effect of tensile strain is so strong, that the top-most portion of the film possessing tetragonal-like crystal structure must orient its long axis of polarization in the plane-of-the-film to accommodate this lattice mismatch and strain. This observation is consistent with piezoresponse force microscopy of the as-grown heterostructures [see Figs. S1(c) and S1(d) in Supplemental Material[41]] and helps explain the diminished remnant polarization values reported herein (Fig. 1) since a considerable fraction of the heterostructure cannot be switched upon application of electric field along the substrate normal.

As stated above, prior modeling approaches to similar systems have suggested that depolarization effects may not be required in these models to accurately predict the properties.

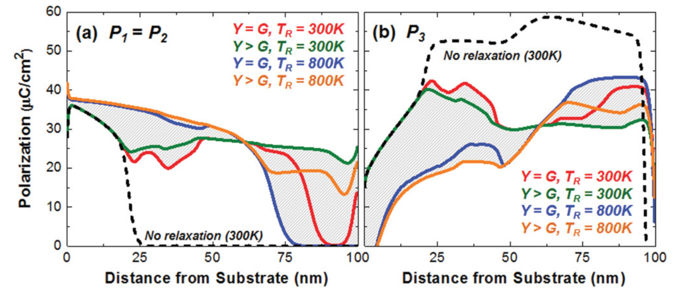

FIG. 3. (Color online) Evolution of (a) in-plane ($P_1 = P_2$) and (b) out-of-plane (P_3) polarization across the thickness of a 100 nm thick compositionally up-graded film at 300 K. For comparison, the same polarization components are calculated for coherently strained films (black dashed line labeled no relaxation). Again results from all four variations of the strain relaxation model are provided including $Y = G$, $T_g = 300$ K (red), $Y > G$, $T_g = 300$ K (green), $Y = G$, $T_g = 800$ K (blue), and $Y > G$, $T_g = 800$ K (orange).

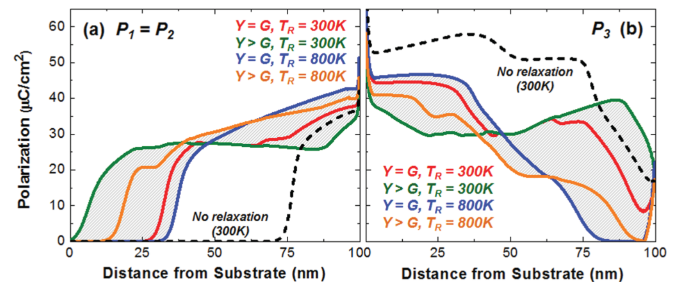

FIG. 4. (Color online) Evolution of (a) in-plane ($P_1 = P_2$) and (b) out-of-plane (P_3) polarization across the thickness of a 100 nm thick compositionally down-graded film at 300 K. For comparison, the same polarization components are calculated for coherently strained films (black dashed line labeled no relaxation). Again results from all four variations of the strain relaxation model are provided including $Y = G$, $T_g = 300$ K (red), $Y > G$, $T_g = 300$ K (green), $Y = G$, $T_g = 800$ K (blue), and $Y > G$, $T_g = 800$ K (orange).

Nonetheless, because of the complexity of the continuously changing polarization throughout the thickness of the film and based on recent reports showing the potential importance of such effects in compositionally graded films[43] we completed additional models including depolarization effects. Such models reveal two main effects: (1) a reduction in the overall value of the polarization in the film and (2) significant flattening in the polarization profile across the thickness for both compositionally up-graded and down-graded heterostructures. Models including depolarization effects predict a nearly uniform polarization through the thickness and an almost identical polarization values for compositionally up-graded and down-graded heterostructures. This is incompatible with both the ferroelectric hysteresis loop measurements and the piezoresponse force microscopy imaging of the domain structures in the heterostructures. It appears that even in a system where the polarization is changing continuously, the fact that these films are "thick" (i.e., much thicker than the screening length of standard oxide electrodes) and that the $PbZr_{1-x}Ti_xO_3$ films possess finite conductivity renders the inclusion of depolarization effects unnecessary.

Returning now to the evolution of the built-in field, the free energy, when supplemented with the boundary conditions and simplified to eliminate the stress components, generates symmetry breaking terms (proportional to odd powers of P_3 and the flexoelectric coefficient) within the thickness that manifest as a built-in field. This flexoelectric contribution to the free-energy density (G_μ) is directly proportional to the flexoelectric coefficient as $G_\mu = -\frac{\mu_{12} P_3}{s_{11}+s_{12}} \frac{\partial u}{\partial x_3}$. To further illuminate the role of flexoelectricity in determining the properties of this system, we performed simulations both with and without the flexoelectric coefficient. These studies reveal that while the flexoelectric coupling does impact the built-in field (and the macroscopic voltage offset), it does not affect the average value of polarization within the film (although it can slightly adjust the values near the film surfaces). As a result, the flexoelectric coupling is found to be responsible for the shifts of the hysteresis loops horizontally, but does not affect the absolute values of the polarization within the material. From the form of the free energy, it is clear that the built-in field requires the presence of both a gradient in the in-plane strain and also the presence of a non-zero polarization along the out-of-plane direction. In the compositionally up-graded heterostructures, the presence of a nonzero P_3 throughout the thickness results in a finite internal bias and it can be estimated that for a system with $\mu_{12} = -1 \times 10^{-10}$ m^3/C, $s_{11} + s_{12} = 5 \times 10^{-12}$ m^2/N, and $\frac{\partial u}{\partial x_3} = -5 \times 10^5$ m^{-1} (or a 5% strain gradient across the 100 nm thick film as in the case of the coherently strained compositionally up-graded heterostructure) the built-in field is $\sim$100 kV/cm, close to the observed value of 200 kV/cm. It should be noted that at the present time, the flexoelectric coefficients and the elastic coefficients are not known accurately enough (both in magnitude and as a function of composition) to calculate a more reliable value theoretically. In the case of compositionally down-graded heterostructures, the lack of an internal bias is also consistent since it has a relaxed rhombohedral layer near the substrate (which reduces the effective strain gradients) and tensile strained tetragonal regions near the surface, which have negligible out-of-plane polarization (but a finite strain gradient). As a result, it is clear that the internal bias in compositionally up-graded and down-graded heterostructures originates from the flexoelectric coupling between the strain gradients and out-of-plane polarization within the film. Thus flexolectricity could play a large effect in nanoscale systems such as thin films which can support large strain gradients. Additionally, our work suggests that these effects may be manifested in counterintuitive manners due to complex strain relaxation and concomitant polarization evolution that occurs in these materials.

V. CONCLUSIONS

In conclusion, we have performed a detailed study of compositionally graded ferroelectric heterostructures using GLD phenomenological models that shed light on the origin of built-in electric fields in these materials. The models indicate that flexoelectric coupling between the out-of-plane polarization and the in-plane epitaxial strain is responsible for the built-in fields and the observed voltage offsets in the hysteresis loops. Additionally, the interplay of structural compatibility between the film and the substrate, strain relaxation, and polarization distribution results in a complex evolution of properties with gradients in composition. Further theoretical and experimental studies are necessary to develop more realistic models of strain relaxation and polarization evolution in the presence of flexoelectricity in these materials. Nonetheless, this work has established the importance of flexoelectricity in compositionally graded ferroelectric heterostructures and shown that through a careful consideration of strain and polarization distributions, large built-in electric fields can be obtained in such systems.

ACKNOWLEDGMENTS

J. K. and L.W.M. acknowledge support from the Office of Naval Research under Grant No. N00014-10-10525. R.V.K.M. and L.W.M. acknowledge the support of the Defense Advanced Research Projects Agency under grant N66001-11-1-4195. J. A. and L.W.M. acknowledge support from the Air Force Office of Scientific Research under grant AF FA 9550-11-1-0073. Experiments were carried out in part in the Materials Research Laboratory Central Facilities, University of Illinois, Urbana-Champaign.

*lwmartin@illinois.edu

[1] J. V. Mantese, N. W. Schubring, and A. B. Catalan, Appl. Phys. Lett. **67**, 721 (1995).
[2] M. Brazier, M. McElfresh, and S. Mansour, Appl. Phy. Lett. **72**, 1121 (1998).
[3] J. V. Mantese, N. W. Schubring, A. L. Micheli, A. B. Catalan, M. S. Mohammed, R. Naik, and G. W. Auner, Appl. Phys. Lett. **71**, 2047 (1997).
[4] N. W. Schubring, J. V. Mantese, A. L. Micheli, A. B. Catalan, and R. J. Lopez, Phys. Rev. Lett. **68**, 1778 (1992).

[5] F. Jin, G. W. Auner, R. Naik, N. W. Schubring, J. V. Mantese, A. B. Catalan, and N. W. Schubring, Appl. Phys. Lett. **73**, 2838 (1998).
[6] S. Zhong, S. P. Alpay, Z.-G. Ban, and J. V. Mantese, Appl. Phys. Lett. **86**, 092903 (2005).
[7] D. Bao, X. Yao, and L. Zhang, Appl. Phys. Lett. **76**, 2779 (2000).
[8] N. Choudhury, L. Walizer, S. Lisenkov, and L. Bellaiche, Nature (London) **470**, 513 (2011).
[9] M. P. Warusawithana, E. V. Colla, J. N. Eckstein, and M. B. Weissman, Phys. Rev. Lett. **90**, 036802 (2003).
[10] S. J. Callori, J. Gabel, D. Su, J. Sinsheimer, M. V. Fernandez-Serra, and M. Dawber, Phys. Rev. Lett. **109**, 067601 (2012).
[11] L. Pintilie, I. Boerasu, and M. J. M. Gomes, J. Appl. Phys. **93**, 9961 (2003).
[12] S. P. Alpay, Z. G. Ban, and J. V. Mantese, Appl. Phys. Lett. **82**, 1269 (2003).
[13] Z. G. Ban, S. P. Alpay, and J. V. Mantese, Phys. Rev. B **67**, 184104 (2003).
[14] G. Ackay, S. Zhong, B. S. Allimi, S. P. Alpay, and J. V. Mantese, Appl. Phys. Lett. **91**, 012904 (2007).
[15] G. Poullain, R. Bouregba, B. Vilquin, G. Le Rhun, and H. Murray, Appl. Phys. Lett. **81**, 5015 (2002).
[16] M. Brazier, M. McElfresh, and S. Mansour, Appl. Phy. Lett. **74**, 299 (1999).
[17] H. K. Chan, C. H. Lam, and F. G. Shin, J. Appl. Phys. **95**, 2665 (2004).
[18] M. Marvan, P. Chvosta, and J. Fousek, Appl. Phys. Lett. **86**, 221922 (2005).
[19] W. Ma and L. E. Cross, Appl. Phys. Lett. **82**, 3293 (2003).
[20] L. Palova, P. Chandra, and K. M. Rabe, Phys. Rev. B **76**, 014112 (2007).
[21] H-X. Cao, V. C. Lo, Z-Y. Li, Sol. State Comm. **138**, 404 (2006).
[22] G. Catalan, B. Noheda, J. McAneney, L. J. Sinnamon, and J. M. Gregg, Phys. Rev. B **72**, 020102(R) (2005).
[23] G. Catalan, L. J. Sinnamon, and J. M. Gregg, J. Phys.: Condens. Matter **16**, 2253 (2004).
[24] D. Lee, A. Yoon, S. Y. Jang, J.-G. Yoon, J.-S. Chung, M. Kim, J. F. Scott, and T. W. Noh, Phys. Rev. Lett. **107**, 057602 (2011).
[25] G. Catalan, A. Lubk, A. H. G. Vlooswijk, E. Snoeck, C. Magen, A. Janssens, G. Rispens, G. Rijnders, D. H. A. Blank, and B. Noheda, Nat. Mater. **10**, 963 (2011).
[26] A. N. Morozovska, E. A. Eliseev, S. V. Kalinin, Long Qing Chen, and V. Gopalan, Appl. Phys. Lett. **100**, 142902 (2012).
[27] R. V. K. Mangalam, J. Karthik, A. R. Damodaran, J. C. Agar, and L. W. Martin [Adv. Mater. (to be published, 2013)].
[28] N. A. Pertsev, A. G. Zembilgotov, and A. K. Tagantsev, Phys. Rev. Lett. **80**, 1988 (1998).
[29] E. A. Eliseev, A. N. Morozovska, G. S. Svechnikov, P. Maksymovych, and S. V. Kalinin, Phys. Rev. B **85**, 045312 (2012).
[30] M. J. Haun, Z. Q. Zhuang, E. Furman, S. J. Jang, and L. E. Cross, Ferroelectrics **99**, 45 (1989).
[31] L.-Q. Chen, *Landau Free-Energy Coefficients, Physics of Ferroelectrics: A Modern Perspective* (Springer-Verlag, Berlin, 2007).
[32] Y. L. Li, S. Y. Hu, Z. K. Liu, and L. Q. Chen, Acta Mater. **50**, 395 (2002).
[33] D. J. Kim, J. Y. Jo, Y. S. Kim, Y. J. Chang, J. S. Lee, J. G. Yoon, T. K. Song, and T. W. Noh, Phys. Rev. Lett. **95**, 237602 (2005).
[34] Y. Watanabe, Phys. Rev. B **57**, 789 (1998).
[35] R. Takayama and Y. Tomita, J. Appl. Phys. **65**, 1666 (1989).
[36] G. Shirane and K. Suzuki, J. Phys. Soc. Jpn. **7**, 333 (1952).
[37] J. Tersoff, Appl. Phys. Lett. **62**, 693 (1993).
[38] J. S. Speck and W. Pompe, J. Appl. Phys. **76**, 466 (1994).
[39] B. Bertoli, E. N. Suarez, J. E. Ayers, and F. C. Jain, J. Appl. Phys. **106**, 073519 (2009).
[40] J. Karthik and L. W. Martin, Phys. Rev. B **84**, 024102 (2011).
[41] See Supplemental Material at http://link.aps.org/supplemental/10.1103/PhysRevB.87.024111 for x-ray reciprocal space maps and piezoresponse force microscopy images of the graded heterostructures.
[42] A. S. Yurkov, JETP Lett. **94**, 455 (2011).
[43] M. B. Okatan, A. L. Roytburd, V. Nagarajan, and S. P. Alpay, J. Phys.: Condens. Matter. **24**, 024215 (2012).